



**SCHOOL OF ADVANCED STUDIES OF THE
ROMANIAN ACADEMY**

DOCTORAL SCHOOL OF CHEMICAL SCIENCES

„Ilie Murgulescu” Institute of Physical Chemistry

IN THE FIELD OF CHEMISTRY

***THE DESIGN AND THE STRUCTURAL STUDY OF
SOME BIOPOLYMER COMPLEXES WITH POTENTIAL
MEDICAL APPLICATIONS***

SUMMARY OF Ph.D. THESIS

Scientific Adviser,

DR. CS I. ANGELESCU DANIEL-GEORGE

PhD Student,

VIȘAN (married TOMA) RALUCA-MARIETA

2024

SUMMARY

Abbreviation list.....	6
THEORETICAL SECTION.....	8
Introduction.....	9
CHAPTER I. INTRODUCTORY NOTIONS.....	11
1.1. The study of biological polymers of carbohydrate type (chitosan, CT)	12
1.2. Phytic acid, PA- a cyclic representative of the polyphosphate class	15
1.3. The design of biomacromolecular complexes based on chitosan.....	18
1.4. Applications of carbohydrate-based complexes in the encapsulation of substances with biological and pharmaceutical relevance (cafeic acid, ferulic acid, quercetin)	21
1.5. The synthesis and production of polyelectrolyte complexes based on chitosan	24
CHAPTER II. EXPERIMENTAL TECHNIQUES IN THE CHARACTERIZATION OF POLYELECTROLYTE COMPLEXES	27
2.1. Dynamic light scattering	28
2.2. Fourier Transform InfraRed spectroscopy	32
2.3. UV-Vis spectroscopy	33
2.4. Fluorescence spectroscopy.....	35
2.5. Atomic force microscopy.....	36
CHAPTER III. MOLECULAR SIMULATIONS TECHNIQUES.....	38
3.1. Molecular dynamics for biologically relevant media	39
3.2. Interaction potentials in molecular dynamics	42
3.3. Boundary conditions, Ewald summation and equilibrium with one reservoir.....	44
3.4. Structural and energetic parameters of interest extracted from molecular dynamics simulations	47
3.5. Moving from an atomistic to a coarse-grained description, compatible with the Martini force field.....	51
EXPERIMENTAL SECTION.....	55
Chapter IV. REMARKABLE PUBLISHED RESULTS	56
4.1. Application of the classical GROMOS force field for computational modelling of phytic acid, quercetin and chitosan chain through an atomistic level of detail	57

4.2. The crosslinking mechanism of chitosan in the presence of phytic acid, revealed by molecular dynamics	66
4.3. A complementary approach of experimental and computational study on the encapsulation of quercetin in the chitosan-phytic acid complex	92
4.4. Granular modeling of phytic acid in the study of ionic cross-linking processes in the constitution of chitosan-based hydrogels.....	119
General conclusions and perspectives.....	151
BIBLIOGRAPHY	157
Annexes	177

Keywords: chitosan-phytic acid, quercetin, molecular dynamics

Introduction

Biopolymers represent a class of natural macromolecules with applicability in the medical field [1]. Chitosan (CT) is an example of a natural polymer, which is extracted from chitin, the main constituent of the exoskeleton of marine organisms [2]. Its versatility contributes to the possibility of functionalizing biomaterials such as microspheres, thin films, nanoparticles or macroscopic gels for studying the release profiles of small molecules, including quercetin (Qe) [3], [4]. Due to the strong protonation in acidic medium of amino groups from glucosamine units, CT chains can associate via electrostatic bonds with physical crosslinkers [5]. Phytic acid (PA) is a type of polyphosphate with circular structure, in which six phosphate groups are grafted through phosphoester bonds onto a cyclohexane ring [6]. The antioxidant, hepatoprotective or anticarcinogenic properties recommend the use of PA in the development of CT-based biomaterials [7], [8].

Starting from these considerations, the current doctoral thesis intitulated „*The design and the structural study of some biopolymer complexes with potential medical applications*” proposes both experimental and computational investigations of the polymorphism of CT and PA-based networks that can capture quercetin, a polyphenol with a wide range of biological characteristics. The main aim of the research directive consists in the molecular mechanism understanding of CT interaction with PA, the conformation adopted by the network, the morphology of the obtained polymeric complexes and the optimization of the encapsulation processes or to facilitate the quercetin transport. Moreover, the molecular mechanisms which are responsible for the crosslinking process have been investigated through an atomistic, respectively coarse-grained level of detail, compatible with the two related force fields, GROMOS 56ACARBO and Martini 2.P. The doctoral thesis includes a theoretical and an experimental section and is divided into four chapters, based on a broad introduction to the study of biopolymer complexes and related original contributions. Chapters I-III include literature data, basic concepts, and expositions of the experimental (DLS, FT-IR, UV-Vis, fluorescence, and AFM) and computational (atomistic/coarse-grained modeling) methods approached to support the original results. The last chapter is dedicated to the remarkable results published in specialized articles.

CHAPTER IV. REMARKABLE PUBLISHED RESULTS

4.1. Application of the classical GROMOS force field for computational modelling of phytic acid, quercetin and chitosan chain through an atomistic level of detail

The initial geometry of CT was generated with the Avogadro package [9] and the topology was taken from the approach proposed by Naumov & Ignatov [10] for carbohydrate structures. The developed polymer model is based on a sequence of four monomer units. In particular, two monomers of CT chain were defined as terminal monomer units and were abbreviated as CHT0 and CHTN, respectively. The abbreviated intermediate monomer units CHTP & CHT contain protonated/deprotonated amino groups. In other words, an N-protonated β -D-glucopyranosamine-2 head unit was modified by adding i) a hydroxyl group to represent the terminal unit, ii) a hydrogen in order to define the CHTN terminal group, or iii) acetylated at the level of $-\text{NH}_2$ group for the ACE monomer. The atomic structures as well as the names assigned to the deacetylated forms are given in the Figure 4.1.

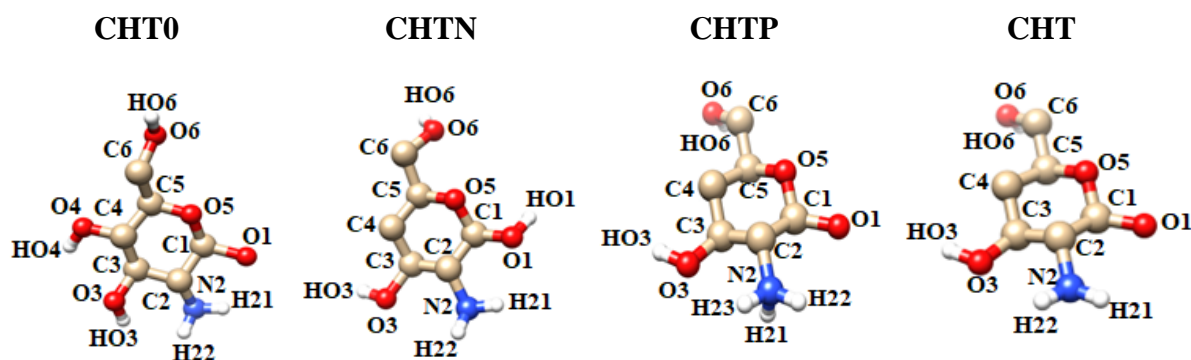


Figure 4.1. Atom numbering for chitosan monomers: terminal units (CHT0 & CHTN) and intermediate units (CHTP& CHT).

The terminal units were always considered electroneutral, while by alternating the other three types of monomers CHT, CHTP or ACE, any desired sequence of CT can be obtained. In Figure 4.2, are illustrated examples of chains with different protonation degrees which were investigated in the coupling mediated by the presence of phytic acid.

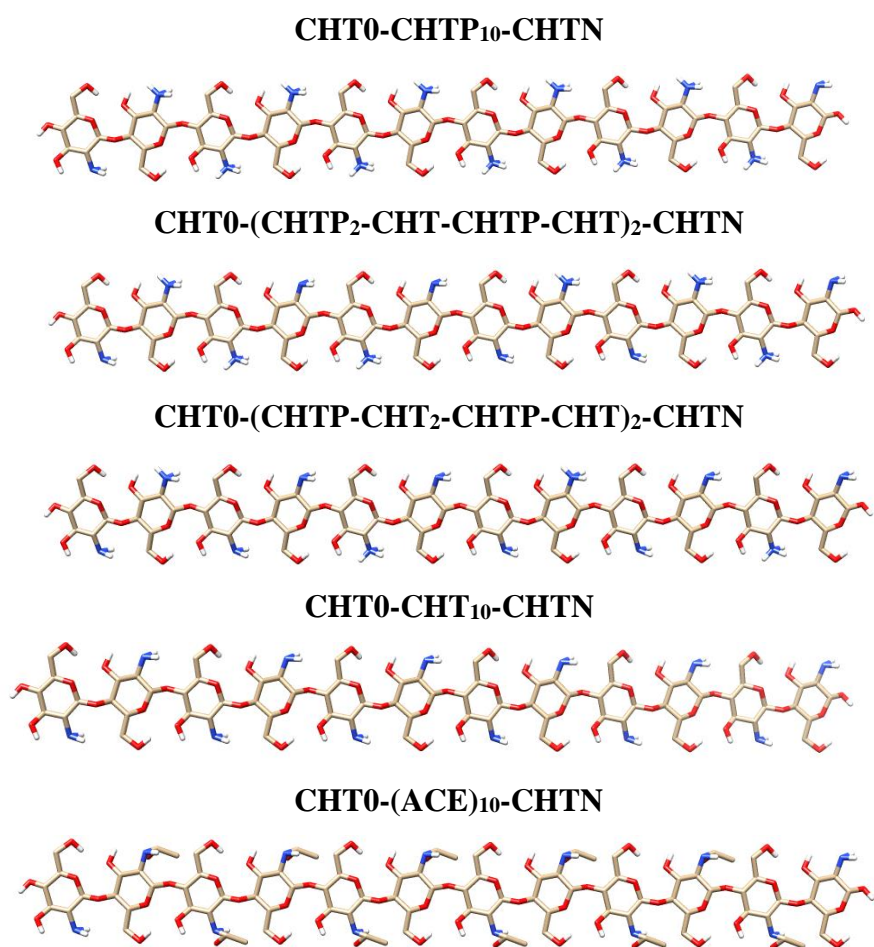


Figura 4.2. The sequence of CT chains. The color code is related to the representing atoms:
C – white/grey, O – red and N – blue.

The inositol plane is rendered using the positions of the carbon atoms: C, C1, C2, C3, C4, C5, which reproduce the chair conformation of the ring. The phosphodiester oxygen atoms O18, O19, O21, O23 and O22 are located in the inositol plane, while the O20 atom is positioned perpendicular to the plane. This structure was optimized using a calculus server named *Automated Topology Builder* (ATB) [11].

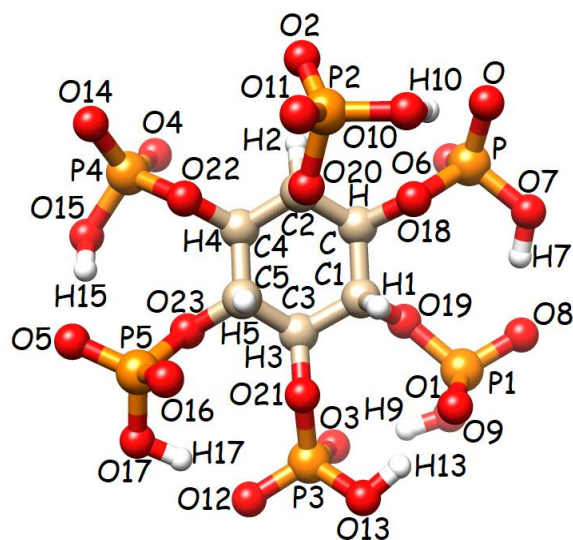


Figure 4.3. The structure of a hexavalent phytate anion and the atom numbering in order to establish the topology of the molecule in the sphere-bond representation.

The computational study of quercetin (Qe) was based on its neutral form representation and the molecule stereochemistry was designed similarly to the atomistic details of PA. Thus, the initial structure was built using Avogadro 1.2.0 which was later used on *Automated Topology Builder* (ATB) to obtain the equilibrium structure and the compatible topology with the mentioned force field. The resulting geometry is shown in Figure 4.4.

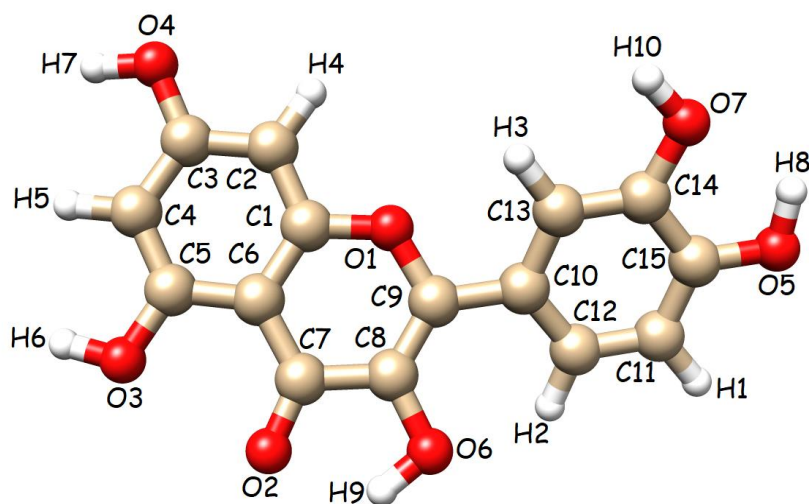


Figure 4.4. The geometry and the atomistic representation of quercetin

4.2. The crosslinking mechanism of chitosan in the presence of phytic acid revealed by molecular dynamics

From an experimental point of view, the synthesis of CT-AF nanoparticles started from the preparation of CT in acetic acid (1%) and phytic acid (1%) stock solutions, respectively. The pH of CT solution was adjusted to 2.6 with a concentrated 1M solution of HCl. The PA solution was filtered using a microfilter with diameter of 0.45 μm and the CT solution was passed through a qualitative filter paper. The final phytate solution was added dropwise to the CT solution using a 10 mL syringe under magnetic stirring (750 rpm) for 30 minutes to obtain the following CT:AF mass ratios (1:1, 3:1, 5:1). Aggregates were formed while stirring and after that were merged and subsequently separated by centrifugation at 5000 rpm for 120 minutes at room temperature. After supernatant removal, the obtained pellets were collected and purified by repeated washing with ultrapure water. Before performing the experiments, samples were redispersed and homogenized using an ultrasonic bath (10 minutes at room temperature) and also using a vertical ultrasonicator with homogenization for 5-15 minutes at the room temperature.

Molecular dynamics simulations are based on an atomistic description of CT chains and PA. In the construction of polymer chains four types of monomer units have been considered, two terminal units with the abbreviation CHT0 and CHTN, and two intermediate units CHTP & CHT. By alternating intermediate units from the constitution of a polymer sequence formed by 12 monomers, systems with different protonation degrees were obtained: 0.83 (all intermediate units were protonated); 0.5 and 0.33 (two symmetric intermediate sequences were random protonated); 0.0 (electrically uncharged system) and ACE (amino groups from intermediate units show acetylations). In the case of a system with the highest protonation degree (0.83) it was not possible to protonate the terminal units due to the restrictions applied to the GROMOS 56ACARBO force field. The structures and abbreviations of the five model systems are presented in Table 4.1.

Tabelul 4.1. The sequence of glucosamine units for a CT chain formed by 12 monomers; a)–d) different protonation degrees 0.83, 0.50, 0.33, 0.00 and acetylated CT; The structures were obtained by adding the following groups $-\text{NH}_3^+$, $-\text{NH}_2$ and $-\text{NHCOCH}_3$ to the C2 atom of the glucosamine unit. The terminal units show only the NH_2 group.

Protonation degree	Sequence
0.83	CHT0-CHTP ₁₀ -CHTN
0.50	CHT0-(CHTP ₂ -CHT-CHTP-CHT) ₂ -CHTN
0.33	CHT0-(CHTP-CHT ₂ -CHTP-CHT) ₂ -CHTN
0.0	CHT0-CHT ₁₀ -CHTN
ACE	CHT0-(CHT-ACE) ₁₀ -CHTN

The computational method involves the random placement of a number of ten CT chains and a variable number of phytic acid molecules (5, 10, 40) in a cubic construction with predetermined dimensions (10 nm x 10 nm x 10 nm). The box was subsequently solvated with approximately 32.000 molecules being compatible with GROMOS 56ACARBO force field. The electroneutrality of the medium was ensured by the addition of Na^+ ions and Cl^- counterions. The simulations were performed under 3D periodic conditions at constant pressure and temperature using the molecular dynamics package GROMACS 4.5.4 [12]. Afterwards a 50.000-step energy minimization took place followed by a 1 ns pre-equilibration in the canonical NVT ensemble. The structural data were extracted from the actual runs and were carried out in a time interval of 150 ns at $T = 300 \text{ K}$ and $p = 1 \text{ atm}$.

Tabel 4.2. The description of the investigated CT-AF systems

System	Number of molecules	Number and type
CHT-PA	Chitosan	Phytic acid Counterions
CHT-083-05	10	5 70 Cl^-
CHT-083-10	10	10 40 Cl^-
CHT-083-40	10	40 140 Na^+
CHT-050-10	10	10 /
CHT-033-10	10	10 20 Na^+
CHT-0-40	10	40 240 Na^+
CHT-ACE-40	10	40 240 Na^+

The theoretical results allowed in-depth conformational analysis of the complexes, hydrogen bonds identification, creating contour maps for minimum distances between the interaction centers (CT-PA), establishing dihedral and torsion angles, calculation of the binding free energy using the Cremer-Pople folding parameters. In the crosslinking process it is highlighted that a single phytate anion can bind up to six CT chains. Also, two phosphate groups can bind a single polymer chain, more precisely, two consecutive glucosamine units. The interaction between the polymer and the crosslinker is an electrostatic one, extremely strong. The conformational analysis is also completed by the formation of hydrogen bonds between the phosphates of myo-inositol and the amino and hydroxyl groups of CT. The circular distribution of the reticulated phosphate groups in the inositol structure determines the polymorphism of the CT-PA network. The electrostatic attraction between these units, amino and hydroxyl groups, influences the approximately isotropic conformational orientations at the junctions. CT allows association with phytate anions through very strong electrostatic bonds forming insoluble complexes. In the case of a neutral and acetylated system it was observed that a few molecules of PA are found in close proximity to the chains. A decrease in the number of hydrogen bonds is highlighted in the case of a completely deprotonated system. In the case of systems with various protonation degrees the ability to form hydrogen bonds increases being possible interactions of the phosphate groups with amino and hydroxyl belonging to two adjacent glucosamine units. The computational results are complemented by a series of experimental investigations of FT-IR spectroscopy and dynamic light scattering for CT-PA biopolymer complexes at different mass ratios for an exhaustive understanding of the molecular arrangement of the crosslinked network.

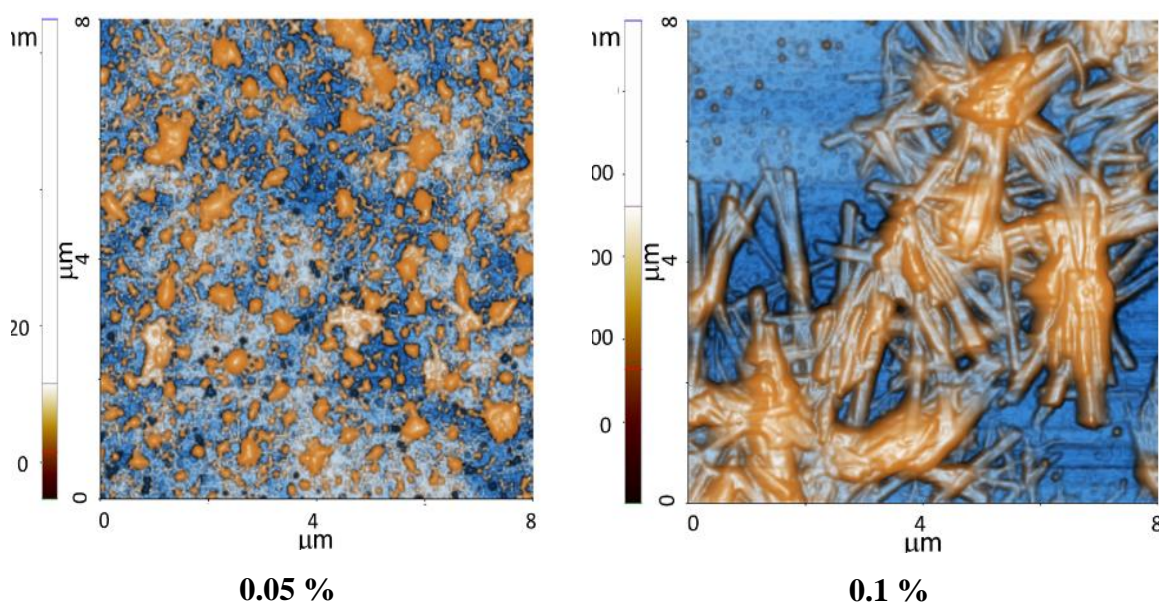
4.3. A complementary approach of experimental and computational study on the encapsulation of quercetin in the chitosan-phytic acid complex

The polymorphism of the investigated network in the previous subsection led both experimentally and computationally to the possibility of embedding in the crosslinked polymer matrix a small hydrophobic molecule from the class of polyphenols, namely quercetin (Qe). The computational study involved a structural analysis based on energetic data extracted from molecular dynamics which showed that the effective encapsulation and retention of quercetin is due to its high ability to associate through hydrogen bonds both with CT chains in the precursor systems as well as in the presence of crosslinking systems.

The theoretical results were supplemented with a series of experimental studies which started from the nanoparticle synthesis procedure as follows: CT was solubilized in an aqueous

solution of acetic acid (1%) and left overnight for equilibration under magnetic stirring at room temperature. Also, a stock solution of PA (1%) was prepared in ultrapure water and left overnight under the previously mentioned conditions. The final concentration of Qe solution (1.5 mg/mL in pure 99% ethanol) was 5×10^{-3} M. This was followed by taking 150 μ L of the stock solution and adding the amounts in three different flasks. After that, the solvent was evaporated. In these samples, the corresponding volumes of solutions with varying concentrations of CT (0.05%, 0.1% and 0.2%) were pipetted followed by sonication for approximately five minutes in an ultrasonic bath at room temperature. 60 μ L of the PA solution was added under magnetic stirring at 750 rpm. After the appearance of the opalescence phenomenon, samples were centrifuged for 30 minutes at 5000 rpm. Subsequently, the samples were washed with ultrapure water and resuspended in 4 mL of assay volume. The supernatants were measured spectrophotometrically and the samples were investigated by different experimental working methods.

The physico-chemical properties of Qe-CT-PA nanoparticles were investigated by fluorescence, infrared, UV-Vis spectroscopies and dynamic light scattering. The experimental studies were complemented by a configurational analysis of the nanoparticles morphology using atomic force microscopy (Figure 4.5). Molecular dynamics simulations were carried out both on CT-Qe and Qe-CT-PA crosslinked systems for a deeper understanding of molecular mechanism.



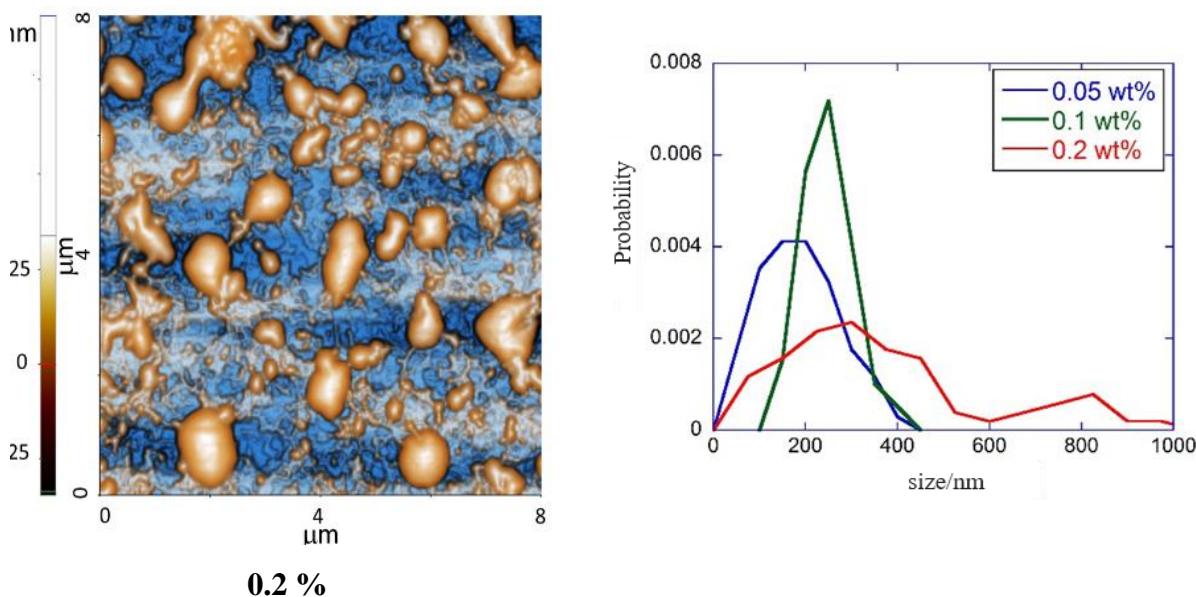


Figure 4.5. Representative images with enhanced phase contrast and particle size distribution of Qe-CT-PA at the indicated CT concentrations.

In order to perform the computational simulations a cubic box was created with the following dimensions: 10 x 10 x 10 nm. Inside it ten CT chains were placed (each chain contains 12 monomeric units with ten protonated intermediate groups). The polymer chains were placed in the box either free or crosslinked with ten molecules of PA. Five Qe molecules were added to both systems whose ability to bind to CT chains was investigated to evaluate the encapsulation efficiency of the formed complex. The placement of Qe was followed by extensive equilibration of the polymer network. On both systems Qe molecules were randomly placed. The box was subsequently solvated with water molecules described using the SPC (extended simple point charge model) force field. Finally Cl^- counterions were added to ensure the electroneutrality of the simulation cell. Molecular dynamics simulations were performed using Gromacs software, version 2019.1.

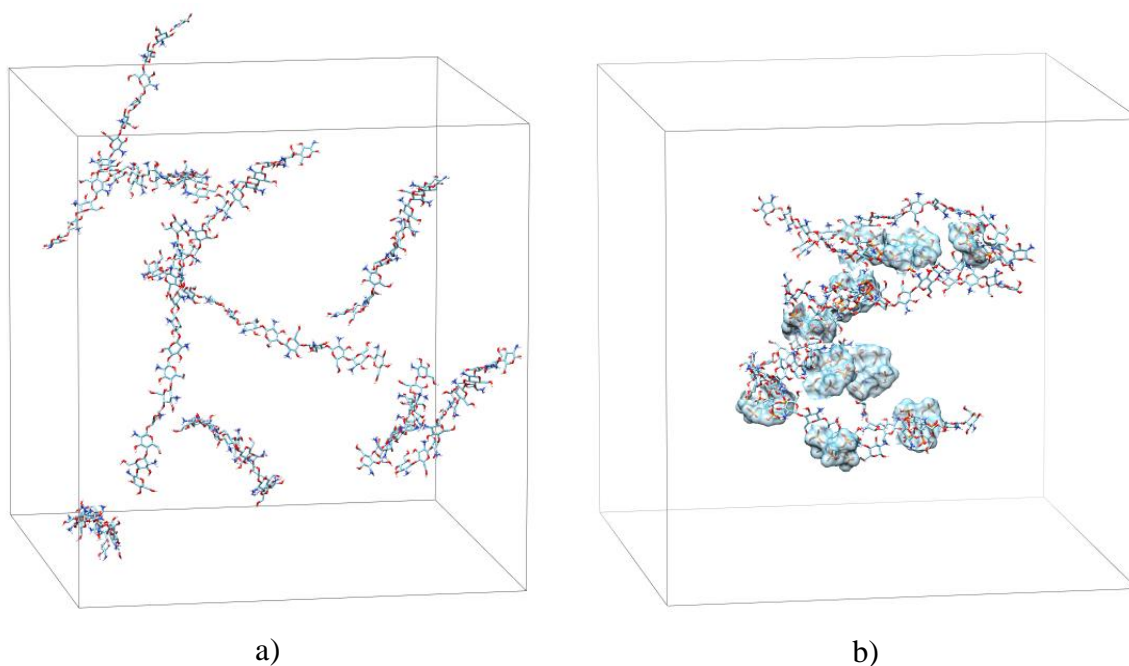


Figure 4.6. The initial configuration of a) free CT chains (represented by sticks) and b) crosslinked PA chains (represented by the surrounding semi-transparent envelope present in the simulation box)

In the case of Qe-CT interaction in aqueous solutions, the hydrogen bonds are mainly established with the hydroxyl and amino groups which belong to the cinnamoyl fragment and glucosamine units. These specific interactions lead to significant immobilization of Qe at the level of the polymer chain. This fact explains the increased anisotropy and vibrational aspect present in the fluorescent behavior and in the embedding efficiency of Qe in the formed network. Atomic force microscopy reveals varied morphologies of the Qe-CT-PA systems, spheres or fibrils obtained at different polymer concentrations. Regarding the encapsulation capacity these nanoparticles show similar characteristics. The CT-PA complex can be used in various studies such as encapsulation, safe and controlled release of active drugs. Both varied content of polymer in the precursor solutions and polarity of the chosen solvent for dialysis do not significantly influence the amount of the antioxidant released. Although, the presence of PA in the systems has a stabilizing role and doesn't influence the binding mode of Qe to the CT chains.

Tabel 4.3. I_T/I_N fluorescence intensity ratio and r anisotropy for 6×10^{-5} M Qe in different media

Samples	I_T/I_N^b	r	
		$\lambda_{em} (450 \text{ nm})^a$	$\lambda_{em} (575 \text{ nm})^b$
PBS buffer :DMSO 1:0.0	1.59 ± 0.03	0.095 ± 0.009	0.084 ± 0.004
PBS buffer :DMSO 1:0.25	3.55 ± 0.03	0.098 ± 0.003	0.082 ± 0.004
0.05 % CT	1.57 ± 0.02	0.303 ± 0.003	0.257 ± 0.003
0.1 % CT	1.01 ± 0.03	0.208 ± 0.002	0.252 ± 0.003
0.2 % CT	0.50 ± 0.02	0.142 ± 0.001	0.242 ± 0.003
0.05 % CT -1.2 mM PA	1.93 ± 0.2	0.390 ± 0.004	0.259 ± 0.004
0.1 % CT - 1.2 mM PA	1.98 ± 0.03	0.376 ± 0.004	0.256 ± 0.003
0.2 % CT - 1.2 mM PA	1.46 ± 0.03	0.317 ± 0.004	0.257 ± 0.003

^a $\lambda_{ex} = 340 \text{ nm}$; ^b $\lambda_{ex} = 370 \text{ nm}$

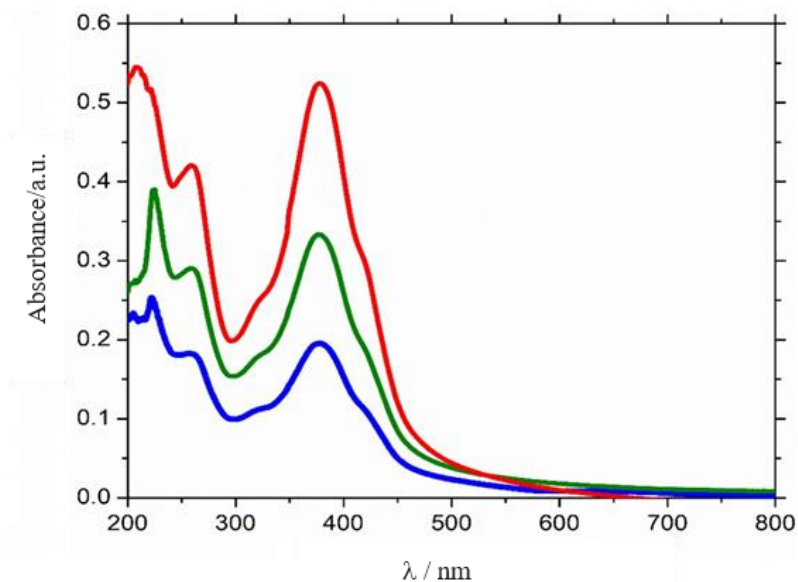


Figure 4.7. UV-Vis spectra of the resulting supernatants from the CT precursor solutions with blue-0.05%, green-0.1% and red-0.2%.

4.4. Coarse-grained modeling of phytic acid in the study of ionic cross-linking processes in the constitution of chitosan-based hydrogels

For a better interpretation of the molecular mechanisms and physico-chemical properties specific to ionic gels a rigorous model for phytate anion and CT compatible with Martini 2.3P force field was parameterized and built. The computational examination consisted in studying the ionic gelation process of a highly protonated CT solution. In the coarse-grained model the non-specific interactions between PA and CT were derived by investigating the structural behavior of a large number of combinations of interaction potentials with the aim of correctly reproducing the structural properties provided based on the atomistic modeling results. Coarse-grained modeling investigates the dynamical and configurational properties of crosslinked CT chains at the level of phosphate units. Also, the pre-existing network topology and the impact of excess crosslinker was also implemented and studied over a longer period of time.

The CT chain is represented by sequences of non-acetylated glucosamine monomers and was possible with the help of the glucose construction developed by Naumov and Ignatov [10], a model based on the GROMOS 56ACARBO force field. The initial CT chain configuration was built using Avogadro package [9] and included a cluster of six protonated residues (a CHTP-type protonated reference unit beta-D-glucopyranose). Two terminal units (CHT0 and CHTN) were added to the protonated groups. PA and CT were simulated individually or together in a 1:3 mass ratio. In both cases the molecules of interest were placed into a 5.5 nm long cubic box in which water molecules (with SPC description) were solvated. A random initial distribution of the constituents was considered and some solvent molecules were replaced by small Na⁺ or Cl⁻ ions to achieve electroneutrality conditions. The molecular dynamics simulations were performed by applying the periodic boundary conditions implemented by the Gromacs software.

The linear polymer fragment was constructed based on the grouping of C and O atoms, from the glucosamine ring and O atoms from the glycosidic bond in the form of coarse-grained representations of B2 bead (polar type, P1, in Martini force field description). The B1 bead (polar type, P2, in Martini force field description) includes the side hydroxyl chain, and another B3 bead (specified as Q0 and P4 in Martini) which associates the opposing hydroxyl and amino moiety with the hydroxyl group in B2 bead. For B3 unit, the specific Martini beads for electrically neutral terminal monomers were P4 and Q0 for +1e⁻ charged beads.

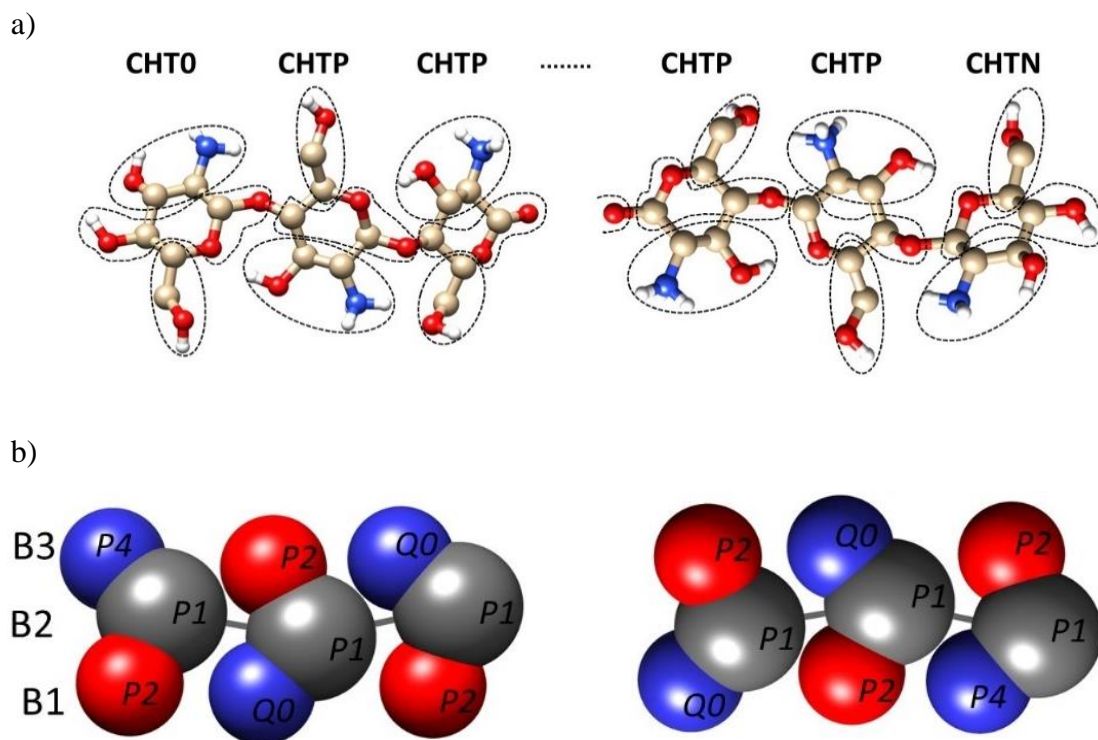


Figura 4.8. All-atom geometric representation and bead assignment in coarse-grained modeling for CT; the dotted areas in a) surround the atoms assigned to a bead, the name of each bead is specified next to it, and in b) the italic font indicates the specific bead for Martini 2.2P model.

The construction of the first type of particle corresponds to the geometric center of two C and O atoms in the ring, plus the P atoms at the level of the corresponding phosphodiester bonds. The core is represented by three spheres named C1-C3. Each of these three beads are *SNa* type in Martini 2.2P force field description. *SNa* is attributed to the loss of polarity of the myo-inositol core when the hydroxyl group is replaced by the phosphodiester bond. For the phosphate beads a *Sqa*-type polar representation was chosen with each bead carrying a negative charge and being positioned out of plane (PO2) or in the inositol plane (PO1, PO3-PO6 beads).

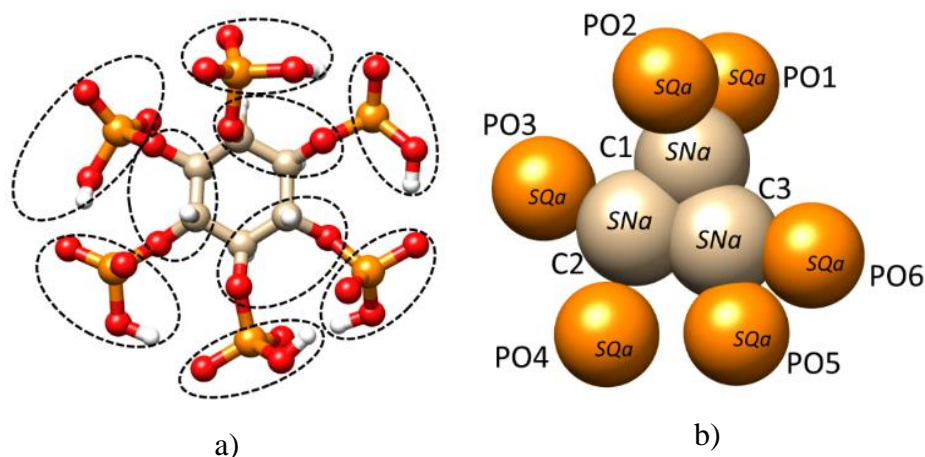


Figura 4.9. a) Geometric representation of all atoms and b) assignment of beads in the coarse-grained model for PA; the dotted areas in a) surround the atoms assigned to a bead, the name of each bead is specified next to it b) the italic font indicates the specific bead for Martini 2.2P model.

GENERAL CONCLUSIONS AND PERSPECTIVES

This PhD thesis proposes a complete scientific research regarding the investigation of biopolymer complexes design based on chitosan and phytic acid with the help of related experimental and computational methods. The molecular dynamics simulations allow the understanding of molecular crosslinking mechanism of chitosan and the impact of functional groups on the morphology of the links mediated by the physical crosslinker. The ability of the phosphate groups to establish hydrogen bonds with the protonated/neutral amino units in the structure of glucosamine units, respectively with the hydroxyl groups positioned on the next monomeric unit allows understanding the molecular mechanism of crosslinking. Also, the possibility of embedding quercetin in the crosslinked polymer matrix was studied computationally and experimentally. It was examined and determined the hydrogen bonds formation in the precursor systems and in the nanoparticles containing polyphenol. The morphology of the nanosystems was analyzed by atomic force microscopy measurements and dynamic light scattering. The fluorescent behavior of quercetin in different solvents, the characteristic anisotropy, the release profile, the encapsulation efficiency of the polyphenol in nanoparticles and the bonds formed in the structure of the complexes were deeply investigated. Depending on the polymer concentration the synthesized complexes can have a spherical or fibrillar shape. Systems based on chitosan and phytic acid form a well-defined and very stable

network allowing the efficient capture of quercetin. For an optimal interpretation of the molecular mechanisms and physico-chemical properties characteristic of ionic gels a rigorous model for chitosan and phytic acid compatible with the Martini 2.3P force field was parameterized. Coarse-grained modeling examines the dynamical and configurational properties of crosslinked CT chains at the level of phosphate units taking into account implementations of atomistic modeling. Also, the topology of the pre-existing network and the impact of excess crosslinker on the chain organization over a longer period of time were studied. The crosslinking model offers a solid interpretation of the interaction mechanisms and physico-chemical properties for the development of ionic gels being also considered an extremely valuable tool for exploring molecular phenomena that occur in other types of polymeric systems.

SELECTIVE BIBLIOGRAPHY

- [1] N. A. Pattanashetti, G. B. Heggannavar, and M. Y. Kariduraganavar, "Smart Biopolymers and their Biomedical Applications," *Procedia Manuf*, 2017, doi: 10.1016/j.promfg.2017.08.030.
- [2] G. Crini, "Historical review on chitin and chitosan biopolymers," *Environmental Chemistry Letters*. 2019. doi: 10.1007/s10311-019-00901-0.
- [3] A. Das, T. Ringu, S. Ghosh, and N. Pramanik, "A comprehensive review on recent advances in preparation, physicochemical characterization, and bioengineering applications of biopolymers," *Polymer Bulletin*, 2022, doi: 10.1007/s00289-022-04443-4.
- [4] S. Nathiya, M. Durga, and T. Devasena, "Quercetin, encapsulated quercetin and its application- A review," *Int J Pharm Pharm Sci*, vol. 6, pp. 20–26, 2014.
- [5] R. M. Visan, A. R. Leonties, L. Aricov, V. Chihaiia, and D. G. Angelescu, "Polymorphism of chitosan-based networks stabilized by phytate investigated by molecular dynamics simulations," *Physical Chemistry Chemical Physics*, vol. 23, no. 39, 2021, doi: 10.1039/D1CP02961D.
- [6] A. S. Sandberg and N. Scheers, "Phytic Acid: Properties, Uses, and Determination," in *Encyclopedia of Food and Health*, 2016. doi: 10.1016/B978-0-12-384947-2.00544-4.

- [7] J. Nissar, T. Ahad, H. R. Naik, and S. Z. Hussain, "A review phytic acid: As antinutrient or nutraceutical," ~ 1554 ~ *Journal of Pharmacognosy and Phytochemistry*, 2017.
- [8] Z. Sang *et al.*, "Comparison of three water-soluble polyphosphate tripolyphosphate, phytic acid, and sodium hexametaphosphate as crosslinking agents in chitosan nanoparticle formulation," *Carbohydr Polym*, vol. 230, p. 115577, 2019, doi: 10.1016/j.carbpol.2019.115577.
- [9] M. D. Hanwell, D. E. Curtis, D. C. Lonie, T. Vandermeersch, E. Zurek, and G. R. Hutchison, "Avogadro: an advanced semantic chemical editor, visualization, and analysis platform. J Chem Inf 4," *J Cheminform*, vol. 4, no. 1, p. 17, 2012, doi: 10.1186/1758-2946-4-17.
- [10] V. S. Naumov and S. K. Ignatov, "Modification of 56ACARBO force field for molecular dynamic calculations of chitosan and its derivatives," *J Mol Model*, vol. 23, no. 8, p. 244, 2017, doi: 10.1007/s00894-017-3421-x.
- [11] A. K. Malde *et al.*, "An Automated Force Field Topology Builder (ATB) and Repository: Version 1.0.," *J Chem Theory Comput*, vol. 7, no. 12, pp. 4026–4037, Dec. 2011, doi: 10.1021/ct200196m.
- [12] M. J. Abraham *et al.*, "GROMACS: High performance molecular simulations through multi-level parallelism from laptops to supercomputers," *SoftwareX*, vol. 1–2, pp. 19–25, 2015, doi: <https://doi.org/10.1016/j.softx.2015.06.001>.

DISSEMINATION OF RESULTS

Papers published in ISI-listed scientific journals whose results were the subject of the doctoral thesis:

1. **Raluca M. Visan**, Anca R. Leonties, Ludmila Aricov, Viorel Chihaiia and Daniel G. Angelescu* “Polymorphism of chitosan-based networks stabilized by phytate investigated by molecular dynamics simulations”, *Physical Chemistry Chemical Physics*, 2021, 23, 22601-22612, **(IF 3.676)**
2. **Raluca M. Visan***, Anca R. Leonties, Mihai Anastasescu and Daniel G. Angelescu, “Towards understanding the interaction of quercetin with chitosan-phytate complex: An experimental and computational investigation”, *Journal of Molecular Liquids*, 2023, 380, 121673, **(IF 6.0)**
3. **Raluca M. Visan & Daniel G. Angelescu***, “Coarse-grained model of phytic acid for predicting the supramolecular architecture of ionically crosslinked chitosan hydrogels”, *Journal of Physical Chemistry B* , 2023, 127, 25, 5718-5729, **(IF 3.3)**

Other papers published in ISI-listed scientific journals

1. Ludmila Aricov, Adina Raducan, Ioana Catalina Gifu, Elvira Alexandrescu, Aurica Precupas, Alexandru Vincentiu Florian Neculae, **Raluca Marieta Visan**, Alina Morosan, Anca Ruxandra Leonties, “The Immobilization of Laccase on Mixed Polymeric Microspheres for Methyl Red Decomposition”, *Coatings*, 2022, 12, 1965, **(IF 3.4)**

Conferences:

1.Raluca Marieta Vişan, Daniel Angelescu, "*An experimental study model and computational design for the chitosan-phytic acid complex*" (oral presentation); CCSAR, Bucharest, november 2021;

2.Raluca-Marieta Vişan, Anca-Ruxandra Leonties, Ludmila Aricov, Daniel-George Angelescu, "*Novel perspective into chitosan-based materials for its broad applications*" (oral presentation), NeXT Chem IV, Bucharest, may 2022;

3.Raluca M. Vişan, Anca R. Leonties, Ludmila Aricov, Mihai Anastasescu and Daniel G. Angelescu, “*The study of a natural antioxidant interaction with a biomaterial* ” (poster); 9th IUPAC International Conference on Green Chemistry (9th ICGC), Athens, september 2022;

4.Raluca M. Vişan*, Anca R. Leonties, Mihai Anastasescu and Daniel G. Angelescu, "*Molecular architecture of biopolymeric complexes*" (oral presentation), MacroYouth 2022, Iaşi, november 2022.

5.Raluca-Marieta Vişan, Daniel Angelescu, „*A coarse-grained model of chitosan for a physical cross-linking pattern*” (poster); ROMPHYSICHEM, Bucharest, september 2023;